Frequency and Beam Reconfigurable Antenna Using Photoconducting Switches

Chinthana J. Panagamuwa, Alford Chauraya, *Member, IEEE*, and J. (Yiannis) C. Vardaxoglou, *Member, IEEE*

***Abstract*—A design for an optically reconfigurable printed dipole antenna is presented. A wideband coplanar waveguide (CPW) to coplanar stripline (CPS) transition is used to feed the balanced printed dipole. Two silicon photo switches are placed on small gaps in both dipole arms equidistant from the centre feed. Light from two infrared laser diodes channelled through fiber optic cables is applied to the switches. With the gaps in the dipole bridged, the antenna resonates at a lower frequency. Measured return loss results that compare well to the simulated values are also presented, showing a frequency shift of nearly 40%. The change in bore-sight gain along with radiation patterns are also presented. Activating each switch individually results in a near 50° shift in beam nulls.**

***Index Terms*—Dipole antenna, frequency control, optical switches, silicon.**

I. Introduction

With the increase in demand for multiband antennas in recent years, reconfigurable active antennas have become an attractive option. A single reconfigurable antenna has the possibility of switching to all the required frequencies, thus eliminating the need for complicated wideband and multiband antenna solutions.

Coplanar waveguide (CPW) and coplanar stripline (CPS) have many advantages in RF circuit design. For example, they allow the easy placement of shunt and series passive and active devices, and have no need for via-holes to connect to the ground plane. Tilley *et al.* [1] presented a CPW-fed CPS dipole antenna with a wideband balun, which was later modified by Kolsrud *et al.* [2] to include varactor diodes for frequency tuning. Many designs have been proposed in the past that use the variable reactance property of varactor diodes, but these are normally accompanied by biasing lines and high biasing voltages [3], [4]. PIN diodes in reconfigurable antennas have also gained in popularity, as they require lower biasing voltages [5], [6]. MEMS are limited by low-power handling capabilities and mechanical failure due to moving parts. All these designs require metallic biasing lines to be attached to the antenna which can interfere with the radiation patterns [2], [5]. Using fiber optic cables instead to activate optical switches have the advantage of being electromagnetically transparent and so do not interfere with the radiation patterns of the antenna [7]. They also provide thermal and electrical isolation between the antenna and the control circuitry. Here we have investigated the effect of the switches on the design of a dipole antenna (balanced feed has been maintained throughout) with a view to achieving the maximum possible frequency shift. In addition, beam null shifting has also been investigated by activating each dipole arm switch individually.

Manuscript received February 15, 2005; revised July 13, 2005. This work was supported in part by Flomerics Ltd. and in part by Antrum Ltd. under contract number ELJFV.

The authors are with the Wireless Communications Research Group, Centre for Mobile Communications Research, Department of Electronic and Electrical Engineering, Loughborough University, Leicestershire, LE11 3TU, U.K. (e-mail: C.J.Panagamuwa@lboro.ac.uk; A.Chauraya@lboro.ac.uk; J.C.Vardaxoglou@lboro.ac.uk).

Digital Object Identifier 10.1109/TAP.2005.863393

II. Silicon Switches

The switches on the antenna are diced from wafers of high resistivity (ρ) silicon ($\rho > 6000\ \Omega \cdot \mathrm{cm}$). When illuminated by light, silicon changes from an insulator state to a near conducting state by creating electron-hole pairs. The photons incident upon the silicon must have enough energy to promote electrons from the valence to the conduction band. Light in the near infrared range is ideal for this process as it strikes a balance between the absorption coefficient and the light penetration depth, which are inversely proportional to each other and related to the wavelength of the light. Removing the light source returns the silicon to its previous state and so the reliability of the switch is governed only by the properties of the light source. Light delivery on silicon wafers for generation and switching of frequency selective surface (FSS) arrays has been extensively studied by Vardaxoglou [8]–[10]. Here, we improve on the model regarding the properties of silicon under optical illumination perpendicular to the direction of travel of the microwave signal.

Intrinsic silicon has an equal free electron and hole density of $1.498 \times 10^{10}/\mathrm{cm}^3$ giving a conductivity of just $0.439 \times 10^{-3}\ \mathrm{S/m}$ [11]. Silicon used in this study is n-type doped with Phosphorus to increase the static conductivity to $16.67 \times 10^{-3}\ \mathrm{S/m}$ At thermal equilibrium the phosphorus doped silicon has a higher density of free electrons than holes. The product of the free electron density and the free hole density is believed to be constant for low dopant densities (i.e., less than 1 dopant atom for 10^6 silicon atoms) [12]. Assuming the carrier mobilities do not change for low dopant densities, the free electron and hole densities that correspond to a static conductivity of $16.67 \times 10^{-3}\ \mathrm{S/m}$ can be found as $e_0 = 7.7 \times 10^{11}/\mathrm{cm}^3$ and $h_0 = 2.9 \times 10^8/\mathrm{cm}^3$, respectively.

These are representative of the initial carrier densities of doped silicon in the dark state. When illuminated with light, an equal number of excess electrons and holes are generated in pairs (electron density e and hole density h), adding to the initial free carrier densities (e_0 and h_0) . Lee *et al.* [13] related the excess free carrier density ($e + h$) to the relative complex

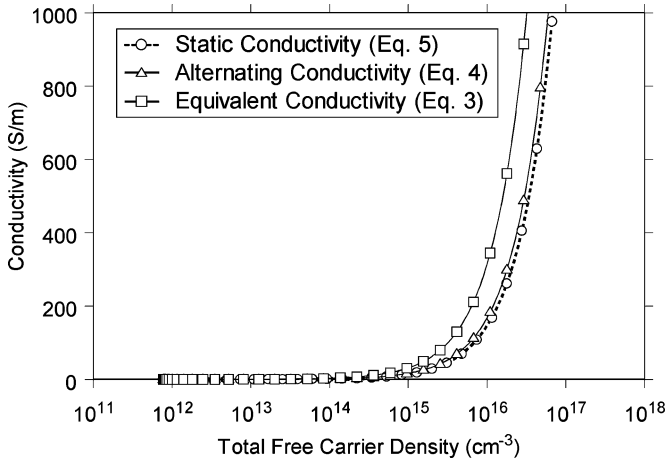

Fig. 1. Change in static, alternating, and equivalent conductivity with increasing silicon total free carrier density at 2 GHz.

permittivity (ε_r) of the semiconductor. Including the initial carrier densities (e_0 and h_0), the equation becomes

$$\varepsilon_r = \varepsilon_L - \sum_{i=e,h} \frac{\omega_{pi_0}^2}{(\omega^2 - v_i^2)} \cdot \left(1 + j\frac{v_i}{\omega}\right) + \frac{\omega_{pi}^2}{(\omega^2 - v_i^2)} \cdot \left(1 + j\frac{v_i}{\omega}\right) \tag{1}$$

where

$$\omega_{pe_0}^2 = \frac{e_0 q^2}{\varepsilon_0 m^*},\ \omega_{ph_0}^2 = \frac{h_0 q^2}{\varepsilon_0 m^*},\ \omega_{pe}^2 = \frac{eq^2}{\varepsilon_0 m^*} \text{ and } \omega_{ph}^2 = \frac{hq^2}{\varepsilon_0 m^*}$$

and q is the charge of an electron; ε_0 is permittivity of vacuum; ε_r is complex relative permittivity of the electron-hole plasma ($\varepsilon_r = \varepsilon' - j\varepsilon''$); ε_L is the relative permittivity of the semiconductor without the plasma; m^* is the effective mass of the charge carrier; and v is the charge carrier collision frequency.

Inserting the complex relative permittivity derived in (1) into Maxwell-Ampère Law [11], the equivalent conductivity (σ_e) of silicon is shown to be made up of a static (σ_s) and alternating (σ_a) part.

$$\begin{aligned} \nabla \times \underline{\mathrm{H}} &= \sigma \underline{\mathrm{E}} + j\omega\left(\varepsilon' - j\varepsilon''\right)\underline{\mathrm{E}} \\ \nabla \times \underline{\mathrm{H}} &= \left(\sigma + \omega\varepsilon''\right)\underline{\mathrm{E}} + j\omega\varepsilon'\underline{\mathrm{E}} \\ \nabla \times \underline{\mathrm{H}} &= \sigma_e \underline{\mathrm{E}} + j\omega\varepsilon'\underline{\mathrm{E}} \end{aligned} \tag{2}$$

where

$$\sigma_e = \text{equivalent conductivity} = \sigma_s + \sigma_a = \sigma_s + \omega\varepsilon'' \tag{3}$$

$$\sigma_a = \text{alternating field conductivity} = \omega\varepsilon'' \tag{4}$$

$$\sigma_s = \text{static field conductivity} = (e+e_0)\,|q|\,\mu_e + (h+h_0)|q|\,\mu_h. \tag{5}$$

μ_e and μ_h are the carrier mobilities for free electrons and holes, respectively. The equivalent conductivity accounts for the conductivity due to free carriers as well as the polarizing effect caused by the applied alternating field. The change in all three conductivities with increasing total free carrier density ($e_0 + h_0 + e + h$) are given in Fig. 1.

The silicon switches were implemented on transmission lines first by Chauraya [14]. Building on these studies, the performance of a microstrip transmission line using a 1 mm × 2 mm × 0.3 mm silicon dice as a switch placed over a 0.25-mm-gap in the line is evaluated in Micro-stripes [15]. An example of a silicon switch used in a transmission line is given in Fig. 2. Here, a 50-Ω transmission line is printed on a Taconic TLY-5 substrate with a dielectric constant of 2.2. The silicon switch is held in place using a silver loaded epoxy.

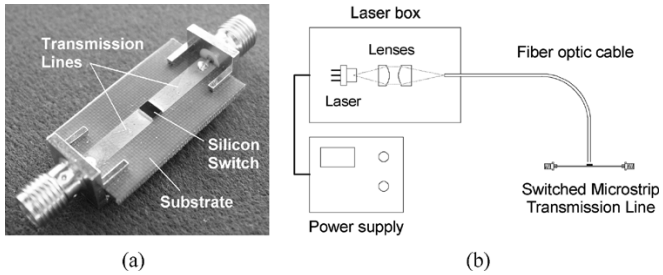

Fig. 2. (a) An example of an optically activated switch in a microstrip transmission line. (b) Experimental setup used for delivering near infrared light.

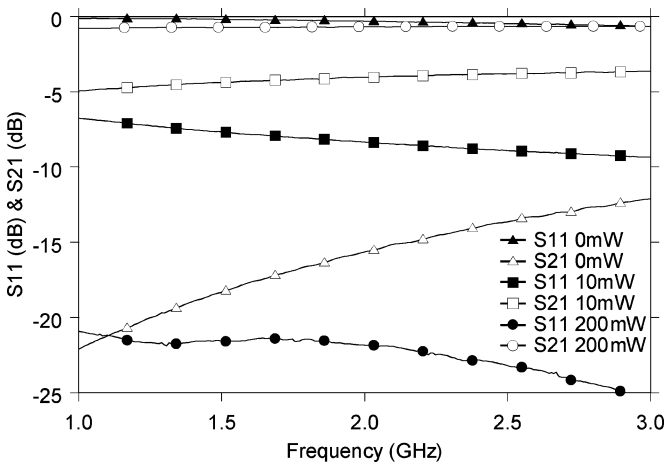

Fig. 3. Measured S-parameters of the switched microstrip line under 0, 10, and 200 mW optical illumination.

In order to simulate the switched transmission line, the derived values for equivalent conductivity (σ_e) plotted in Fig. 1 and their corresponding real permittivity (ε') values are used to define the properties of the silicon dice. The simulated S-Parameter results are compared with measured results obtained by varying the optical power incident on the silicon between 0 and 200 mW. By matching simulated and measured S-Parameter results, each optical power used is assigned equivalent conductivity and permittivity values that can be used in a simulation environment. The measured S-Parameters for the switched line under 0, 10, and 200 mW are given in Fig. 3. At 2 GHz, the switch provides an isolation of 15 dB and an insertion loss of just 0.68 dB with 200 mW of optical power.

The equation given in (1) assumes a uniform carrier generation throughout the silicon. However, the light intensity decreases with increasing penetration depth, less free-carriers are generated in the bulk of the silicon creating a conductivity gradient in the cross section. This was simulated by using a number of layers of silicon, each stacked on top another and each with a higher conductivity than the previous. This complex design significantly increased the simulation time with no improvement in the results and so was deemed to be unnecessary.

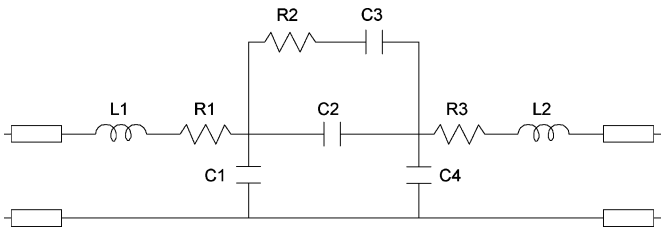

Fig. 4. Lumped element equivalent circuit of the silicon switch.

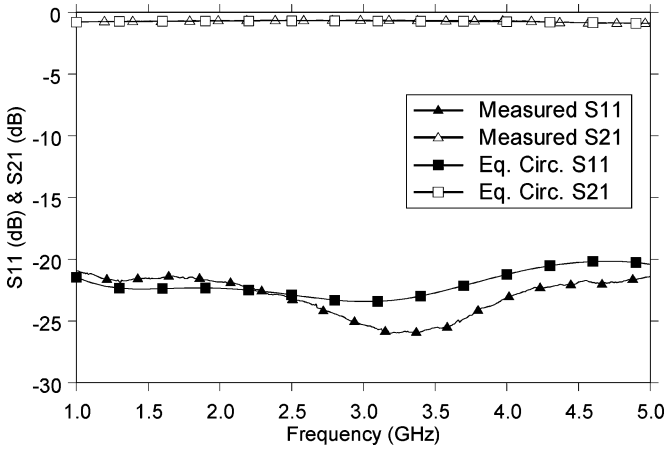

Fig. 5. Measured S-parameters at 200 mW compared to those obtained from the equivalent circuit.

A lumped element equivalent circuit representing the silicon switch (Fig. 4) in a microstrip transmission line has been developed through first principles. Building on the equivalent circuit of a gap in a transmission line (three capacitors C1, C2, C4), additional components are included to account for the photoconducting effect of the silicon, namely R2 and C3. Series inductors (L1 and L2) and resistors (R1 and R3) are added to account for losses in the switch. In order to maintain some symmetry in the switch, C1 is identical to C4, R1 to R3, and L1 to L2. Lumped element circuits in the literature [16], [17] cover microstrip lines printed on a silicon substrate and so differ from this design as there is no conduction through the dielectric here.

The values of the lumped elements are tuned in order to match measured S-Parameters under optical illumination varying from 0 to 200 mW. For illustration purposes, the comparison between the measured and equivalent circuit S-parameters is given in Fig. 5. Analysis of a number of such graphs shows with increasing optical power, the gap capacitances (C2, C3) increase while the gap resistances (R1, R2, R3) decrease, indicating it is a capacitive switch. Silicon oxide used for passivating the switch unfortunately degrades the ohmic contact between the silicon and the copper tracks, thus, reducing dc conductivity. However, at frequencies above 1 GHz the effect of this is not observed.

III. Switched Dipole Antenna

The schematic of the dipole antenna is shown in Fig. 6(a) along with a photograph in Fig. 7. It is printed on 1.17-mm-thick TLY-5 substrate that has a dielectric constant (ε_r) of 2.2. There is no ground plane on the underside of the printed dipole, allowing the antenna to radiate above and below the substrate. The antenna is fed at the CPW using a 50-Ω SMA connector.

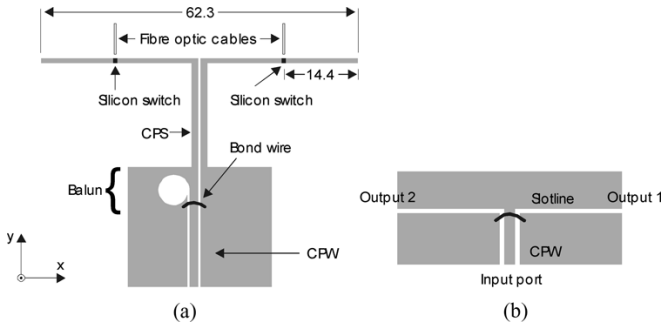

Fig. 6. (a) Optically reconfigurable CPS dipole antenna (dimensions given in millimeters). (b) CPW-Slotline T-junction.

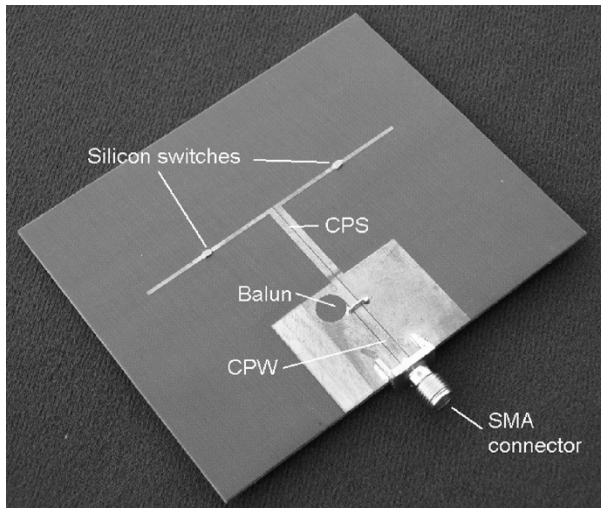

Fig. 7. Photograph of the switched dipole antenna.

The CPW is an unbalanced transmission line but since the dipole is a balanced antenna, a transformation of the input signal is required. The circular balun is used to convert the unbalanced CPW to a balanced CPS [18], [19]. The balun is based on a CPW to slotline T-junction shown in Fig. 6(b) [20]. If output 2 is terminated in an open circuit, there is a complete transfer of current from the CPW to the slotline leaving at output 1. Current in the centre feed of the CPW flows directly onto the top half of the slotline and the backward currents on the ground planes of the CPW combine through the bond wire to form the current on the bottom half of the slotline, thus transforming the CPW mode to a slotline mode. Finally, reducing the width of the slotline creates the CPS. In the antenna structure, the circular stub acts as an open circuit with a non uniform impedance, giving a greater bandwidth match. Simulations of two back-to-back transitions show an insertion loss better than 1.5 dB in the switching range of the dipole antenna.

The dipole resonates when its length is equal to $\lambda_{\text{eff}}/2$ where λ_{eff} is the effective wavelength. λ_{eff} is given by $\lambda_0/\sqrt{\varepsilon_{\text{eff}}}$ where λ_0 is the wavelength in free-space and ε_{eff} is the effective dielectric constant. Although the effects of dielectric loading cannot be ignored, the absence of a ground plane under the antenna reduces the value of ε_{eff} close to 1.2. The dipole is printed with two gaps, each one 14.4 mm from the end of each arm. 1 mm $\times$ 1 mm $\times$ 0.3 mm silicon dice are then placed over the gaps and are held in place using silver loaded epoxy, which ensures good

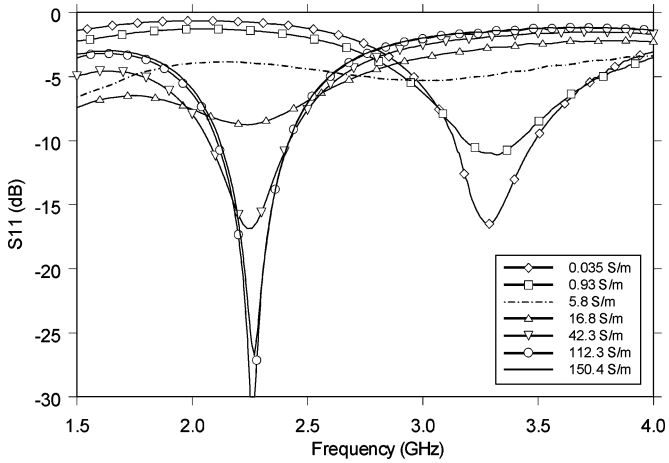

Fig. 8. Simulated change in return loss with increasing silicon conductivity.

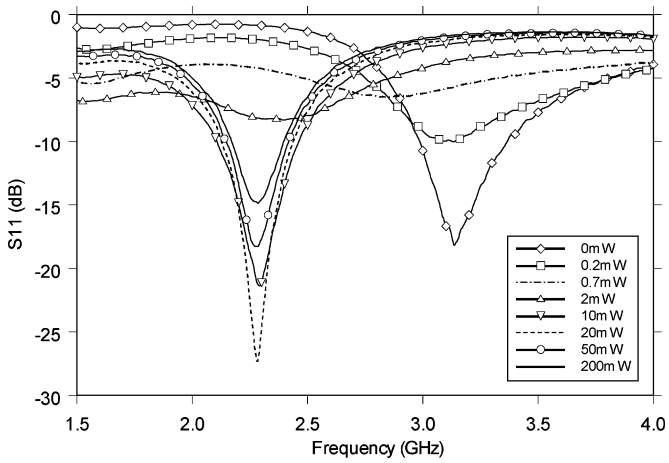

Fig. 9. Measured change in return loss with increasing optical illumination.

contact between the copper and silicon. Two 980-nm lasers operating at 200 mW (maximum output) are coupled to two glass fiber optic cables, which are then angled over the silicon wafers using plastic clamps. When both switches are turned off, the silicon acts as an insulator and so the dipole resonates at its shorter length of 33.5 mm. When both lasers are operating at 200 mW, the silicon conducts and the gaps are bridged, increasing the dipole arm lengths to 62.3 mm and hence reducing the resonance frequency.

IV. Results

A. Frequency Shifting

The simulated change in Return Loss as the conductivity is increased from the off state is shown in Fig. 8. Measured return loss results compare well with those obtained from simulations and are shown in Fig. 9. From both switches on to both switches off, the resonant frequency shifts from 2.26 GHz to 3.15 GHz. This is a shift of 39.4%. The -10 dB bandwidth is 9.5% for the on and 13.4% for the off states.

With the gradual increase in optical power illuminating the switches, the match at 3.15 GHz begins to deteriorate. At 0.7 mW, the resonance has shifted to 2.7 GHz but the match

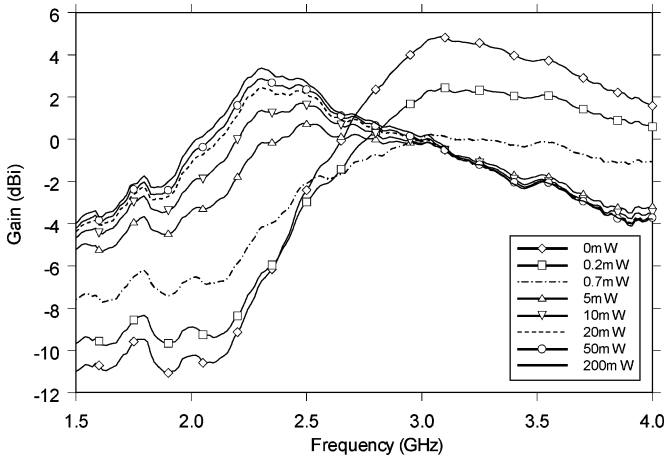

Fig. 10. Change in measured boresight gain with increasing optical illumination.

is poor. Further increase in optical power to 20 mW gives a good match at 2.26 GHz and the shift in frequency is complete. Although the match at 2.26 GHz degrades slightly, the increase in optical power from 20 to 200 mW sees an improvement in the efficiency of the silicon switch. As seen in Fig. 10, this translates to a higher antenna efficiency giving an increase in the boresight gain of 1 dBi at 2.26 GHz. There is only a 0.5-dBi increase in gain when the optical power is changed from 50 to 200 mW and so the antenna could be operated at lower optical powers with only a slight compromise in performance.

There is a clear shift in antenna gain as it switches from both on to both off, with gain changing from 2.9 to 4 dBi. The ripples on the measurements are attributed to the limitations of the anechoic chamber. The difference in gain at 2.26 GHz and at 3.15 GHz between both on and both off states are about 10 and 5.3 dBi, respectively.

Previous work by the author using a dipole with a different feed and a smaller frequency shift [7] has shown that with 200 mW of optical power, the dipole behaves very similar to a full length dipole (62.3 mm long) in terms of resonance frequency and gain. Further increase in optical power causes electron-hole recombination processes that are more prevalent in high free carrier densities to become more active. They immediately recombine electrons freed by the increased photons and thus hamper any further increase in silicon conductivity. Therefore, beyond 200 mW no further noticeable increase in gain is observed.

The resonance of a shorter length dipole (33.5 mm) is slightly higher than that of a switched dipole in the off state. This is due to the capacitive loading effect introduced by the silicon dice. Prior to fixing the silicon dice in place, the dipole behaves similar a 33.5-mm-long dipole. A thorough investigation was carried out to establish the maximum frequency shift while the match was kept below -10 dB. Positioning the switches closer to the antenna feed improves the shift but at the expense of the return loss. The optimum distance for each switch from the ends of the dipole was 14.4 mm.

The measured and simulated E-plane radiation patterns for both operational states are shown in Fig. 11. There is good correlation between measured and simulated patterns. When both

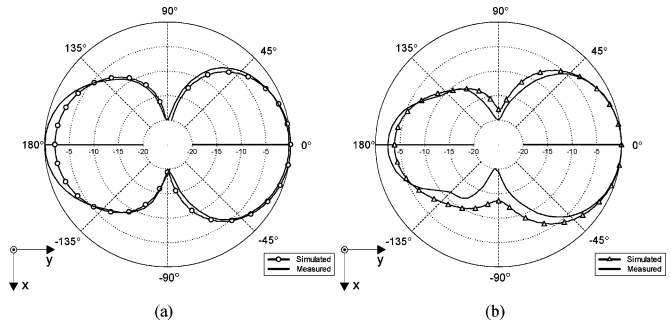

Fig. 11. Measured and simulated E-plane radiation patterns for the printed antenna with both switches (a) ON and both switches (b) OFF.

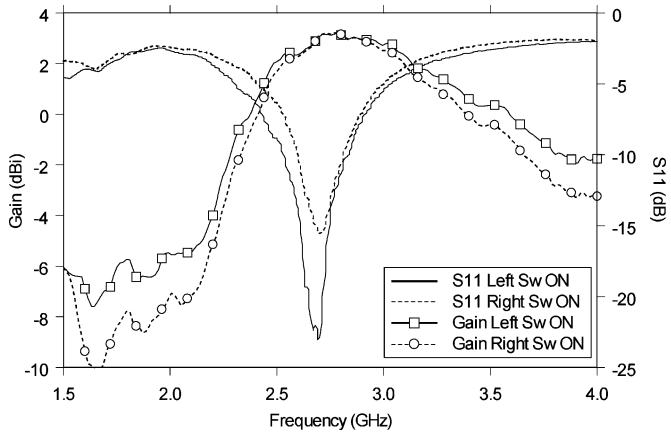

Fig. 12. Measured return loss and boresight gain for the antenna when switches are activated individually.

switches are on or off, the patterns conform well to the typical figure-of-eight patterns expected from a standard half wavelength dipole and they all have very wide beam widths. Comparing both switches on with both switches off, the forward E-plane pattern shapes are very similar indicating that the activation of the switches are not having a detrimental effect on the radiation patterns. The slight change in the reverse pattern is due to interaction with the CPW ground plane, which is more pronounced in the off state because the width of the CPW ground plane is comparable to the length of the dipole.

B. Null Shifting

In addition to these standard modes of operation, each side of the dipole was switched on individually and return loss and gain measurements taken. These are presented in Fig. 12. When only the right switch is on the antenna resonates at 2.70 GHz and with just the left switch on, it resonates at 2.69 GHz. These are frequency shifts of 19.4% and 19.0%, respectively, from the on state. For right switch on and left switch on, the -10 dB bandwidths are 8.8% and 11.3%, respectively. When only one switch is used, the antenna resonates in between the other two extremes and this is also reflected in the gain maxima. The boresight gain here is about 3.1 dBi.

Individual operation of the silicon switches creates an offset feed as one dipole arm becomes longer than the other. Fig. 13 shows how the E-Plane pattern rotates to the left when only the left switch is activated and conversely how it rotates to the right

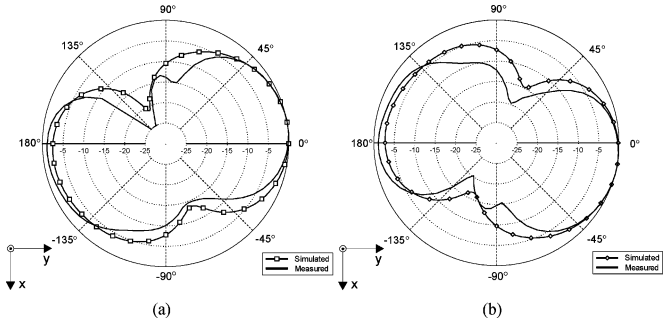

Fig. 13. Measured and simulated E-plane radiation patterns for the printed antenna with (a) only left switch ON and (b) only right switch ON.

when only the right switch is operated. In both these operational states, the resonance frequency is fixed close to 2.7 GHz. When shifted right, the maximum gain is 12° off boresight and when shifted left, the maximum gain is 7° off boresight. This mismatch is due to the asymmetry in the balun and CPW ground planes with respect to the dipole arms. A much larger shift of about 50° in the dipole pattern nulls is observed when the silicon switches are activated alternatively.

V. Conclusion

An optically reconfigurable CPW-fed CPS dipole antenna has been successfully designed and tested. A frequency shift of 39.4% is achieved from both switches on to both switches off. The antenna exhibits ideal forward E-plane radiation patterns and good boresight gain during both switches on and both switches off operation. In addition, switching on of just one switch results in a resonance in the middle of the two extremes and is accompanied by a boresight gain of 3.1 dBi. Switching between arms, the direction of maximum gain shifts by 19° maintaining the same resonance frequency. There is also a much larger shift of about 50° in the E-plane pattern nulls. The antenna can be switched from 2.26 GHz to 2.7 GHz to 3.15 GHz, all the while maintaining good match and gain. In fact, using the different switching combinations, a -7 dB or better S11 with a gain better than 1 dBi can be achieved from 2.1 GHz through to 3.6 GHz. No adverse effects due to fiber optic cables or the silicon wafers were observed.

References

[1] K. Tilly, X.-D. Wu, and K. Chang, "Coplanar waveguide fed coplanar strip dipole antenna," *Electron. Lett.*, vol. 30, pp. 176–177, 1994.

[2] A. T. Kolsrud, M.-Y. Li, and K. Chang, "Dual-frequency electronically tunable CPW-fed CPS dipole antenna," *Electronics Letters*, vol. 34, pp. 609–611, 1998.

[3] J. M. Carrère, R. Staraj, and G. Kossiavas, "Small frequency agile antennas," *Electron. Lett.*, vol. 37, pp. 728–729, 2001.

[4] Y. Turki and R. Staraj, "CPW-fed frequency-agile shorted patch," *Microw. Opt. Technol. Lett.*, vol. 25, pp. 291–294, 2000.

[5] C. Luxey, L. Dussopt, J.-L. Le Sonn, and J.-M. Laheurte, "Dual-frequency operation of CPW-fed antenna controlled by *pin* diodes," *Electron. Lett.*, vol. 36, pp. 2–3, 2000.

[6] F. Yang and Y. Rahmat-Samii, "Patch antenna with switchable slot (pass): Dual-frequency operation," *Microw. Opt. Technol. Lett.*, vol. 31, pp. 165–168, 2001.

[7] C. J. Panagamuwa and J. C. Vardaxoglou, "Optically reconfigurable balanced dipole antenna," in *12th Int. Conf. Antennas Propagation*, vol. 1, Apr. 2003, pp. 237–240.

[8] J. C. Vardaxoglou, "Optical switching of frequency selective surface bandpass response," *Electron. Lett.*, vol. 32, pp. 2345–2346, 1996.

[9] ——, "Optical switching and generation of periodic arrays and FSS," in *Int. Conf. Electromagnetics Advanced Apps.*, 1997, pp. 51–56.
[10] D. S. Lockyer, J. C. Vardaxoglou, and M. J. Kearney, "Transmission through optically generated inductive grid arrays," *IEEE Trans. Microw. Theory Tech.*, vol. 47, pp. 1391–1397, Jul. 1999.
[11] C. A. Balanis, *Advanced Engineering Electromagnetics*. New York: Wiley, 1989, pp. 63–81.
[12] M. S. Tyagi, *Introduction to Semiconductor Materials and Devices*. New York: Wiley, 1991, pp. 69–73.
[13] C. H. Lee, P. S. Mak, and A. P. DeFonzo, "Optical control of millimeter-wave propagation in dielectric waveguides," *IEEE J. Quantum Electron.*, vol. 16, no. 3, pp. 277–288, 1980.
[14] A. Chauraya, D. S. Lockyer, Y. L. R. Lee, and J. C. Vardaxoglou, "A study of optically tuned metallodielectric photonic band gap array and patch antenna," in *11th Int. Conf. Antennas Propagation*, vol. 2, Apr. 2001, pp. 492–496.
[15] *Release 6.5 Micro-Stripes Reference Manual: Issue 1*, Flowmerics Ltd., 2004.
[16] I. L. Andersson and S. T. Eng, "Phase and amplitude characteristics of InP:Fe modified interdigitated gap photoconductive microwave switches," *IEEE Trans. Microw. Theory Tech.*, vol. MTT-37, pp. 729–733, Apr. 1989.
[17] S. S. Gevorgian, "Design considerations for an optically excited semiconductor microstrip gap at microwave frequencies," *Inst. Electr. Eng. Proc., Part J: Optoelectron.*, vol. 139, no. 2, pp. 153–157, 1992.
[18] C. –H. Ho, L. Fan, and K. Chang, "Broad-band uniplanar hybrid-ring and branch-line couplers," *IEEE Trans. Microw. Theory Tech.*, vol. MTT-41, pp. 2116–2125, Dec. 1993.
[19] K. C. Gupta, R. Garg, I. Bahl, and P. Bhartia, *Microstrip Lines and Slotlines*, 2nd ed. Boston, MA: Artech House, 1996.
[20] H. Ogawa and A. Minagawa, "Uniplanar MIC balanced multiplier – A proposed new structure for MIC's," *IEEE Trans. Microw. Theory Tech.*, vol. MTT-35, pp. 1363–1368, Dec. 1987.

Chinthana J. Panagamuwa was born in 1977 in London, U.K. He received the M.Eng. degree in electronic and electrical engineering in 2000, and the Ph.D. degree in optically controlled microwave switches and frequency reconfigurable antennas in 2005, both from Loughborough University, Leicestershire, U.K.

His main research interests are in optical control of silicon switches, frequency and beam reconfigurable antennas, and low SAR handset antennas. He is currently a Research Associate at Loughborough University investigating low SAR and high efficiency ferrite loaded antennas for mobile handsets.

Alford Chauraya (S'99–M'02) was born in 1970 in Zimbabwe. He received the B.Tech. (Hons.) degree in electrical engineering and the M.Sc. degree in communications engineering from University of Zimbabwe in 1994 and 1996, respectively.

He is currently working toward the Ph.D. degree in wireless communications engineering at Loughborough University, Leicestershire, U.K. Since 2002, he has worked as an Research Associate with the Wireless Communications Research Group, Department of Electronic and Electrical Engineering, Loughborough University. His current area of research is in the field of electromagnetic band gap (EBG) structures with emphasis on reconfigurable antenna applications and optically tunable microwave devices. His work involves the design, analysis, and measurement of various optically controlled systems for microwave and mmwave applications.

J. (Yiannis) C. Vardaxoglou (M'87) received the B.Sc. degree in mathematics (mathematical physics) and the Ph.D. degree from the University of Kent, Canterbury, U.K., in 1981 and 1985, respectively.

In January 1988, he was appointed Lecturer in Communications with the Department of Electronic and Electrical Engineering, Loughborough University of Technology, Leicestershire, U.K. He was promoted to the position of Senior Lecturer in January 1992, and in 1998, was appointed Professor of Wireless Communications. He holds the Chair of Wireless Communications at Loughborough University and is the Founder of the Centre for Mobile Communications Research (CMCR). He established the Wireless Communications Research (WiCR) group at Loughborough University. He also heads the Centre for Mobile Communications Research. He has pioneered research, design, and development of frequency selective surfaces (FSS) for communication systems and has commercially exploited a number of his innovations. He has been active in the analysis and design of small low-specific absorption rate (SAR) material loaded antennas for mobile telephony and electromagnetic band gap (EBG) structures for subsystem applications. His current research interests include array antennas, FSS, radomes, leaky wave resonant antennas, optical control of microwaves and devices, periodic surfaces and EBG/AMC/LH materials, and material-loaded mobile telephone antennas. He has served as a consultant to various industries, holds three patents, and is the Technical Director of Antrum Ltd. He has published over 130 refereed journals and conference proceeding papers and has written a book on FSS.

Dr. Vardaxoglou is currently the Chairman of the executive committee of the IEE's Antennas and Propagation Professional Network and he chairs the IEEE's distinguish lecturer program of the Antennas and Propagation society. He Chairs the Executive Committee of Metamorphose, EU FP6 Network of Excellence of Metamaterials. He chaired the 1st and 2nd IEE Antenna Measurements and SAR (AMS'02 and AMS'04) conferences and has been on the organizing committee of the 2001 and 2003 IEE International Conferences on Antennas and Propagation. He was the general Chair of the 1st Loughborough Antennas and Propagation Conference (LAPC'05).